Supporting information

Enhancing photoelectrochemical performance of Bi_2MoO_6 photoanode by ferroelectric polarization regulation

Zhongshuai Xie,[a] Zongyang Cui,[a] Jiafeng Shi,[a] Cheng Lin,[a] Kan Zhang,[a] Guoliang Yuan*,[a] and Jun-Ming Liu[b]

[a]School of Materials Science and Engineering, Nanjing University of Science and Technology, Nanjing 210094, P. R. China

[b]National Laboratory of Solid State Microstructures, Collaborative Innovation Center of Advanced Microstructures, Nanjing University, Nanjing 210093, P. R. China

* Corresponding author: G. L. Yuan; E-mail: yuanguoliang@njust.edu.cn

Table S1. A survey of literature regarding photoelectrochemical performance of Bi_2MoO_6 photoelectrodes.

Morphology	Light source	Electrolyte	Photocurrent density	Reference
Film	300 W Xe lamp (150 mW/cm^{-2}) γ>420 nm	0.1 M KCl	<10 μA/cm^2 @ 0.8 $V_{Ag/AgCl}$	1
Nanowall	300 W Xe lamp (50 mW/cm^{-2})	0.5 M Na_2SO_4	75 μA/cm^2 @ 0.9 $V_{Ag/AgCl}$	2
Nanorod array	300 W Xe lamp γ>420 nm	0.1 M Na_2SO_4	12 μA/cm^2 @ 0.8 V_{SCE}	3
Nanosheet	AM 1.5G(100 mW/cm^{-2})	0.5 M Na_2SO_4 (pH 6.5)	<100 μA/cm^2 @ 1.23 V_{RHE}	4
Nanosheet	AM 1.5G(100 mW/cm^{-2})	0.1 M Na_2SO_4 (pH 6.8)	120 μA/cm^2 @ 1 V_{RHE}	5
Nanopillars	AM 1.5G(100 mW/cm^{-2})	0.5 M Na_2SO_4 (pH 6.8)	250 μA/cm^2 @ 1.23 V_{RHE}	This work

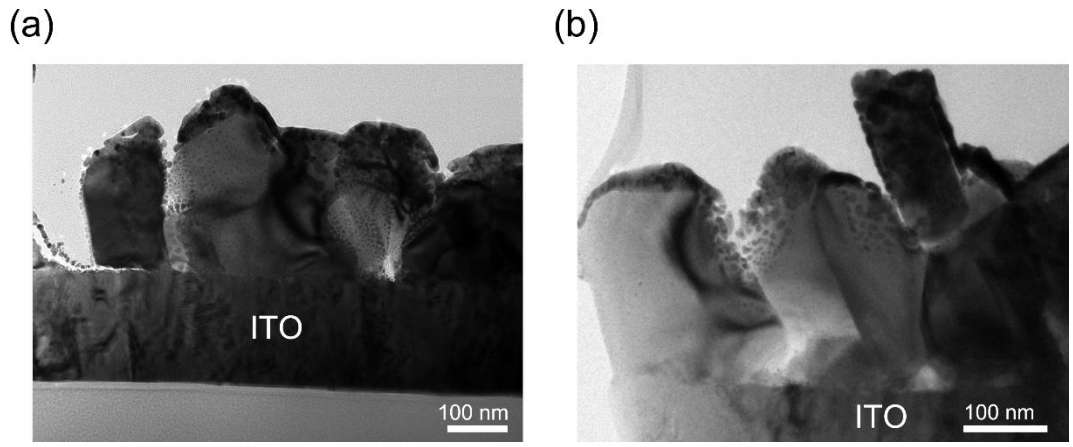

Fig. S1 Cross-sectional TEM images of Bi_2MoO_6 nanopillars.

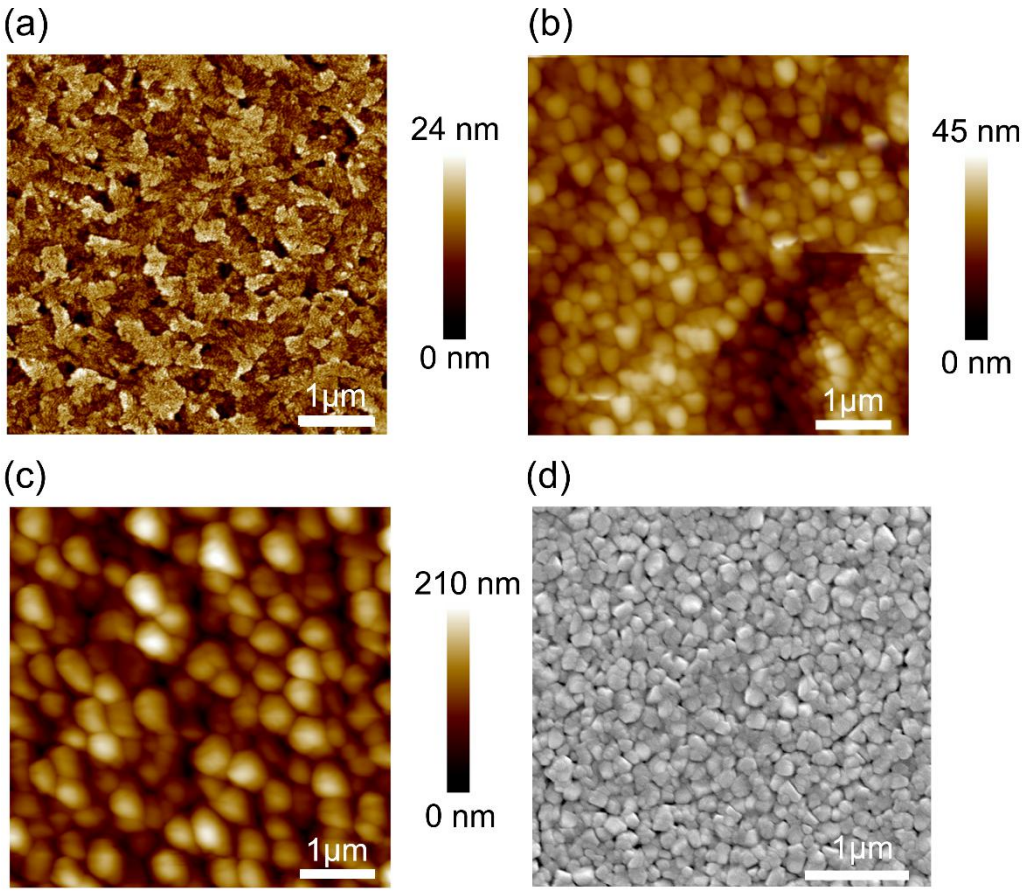

Fig. S2. AFM surface topographies of (a) ITO film, (b) the flat film and (c) nanopillars of Bi_2MoO_6 grown on the ITO-coated glass substrate, respectively. (d) SEM image of the flat Bi_2MoO_6 film.

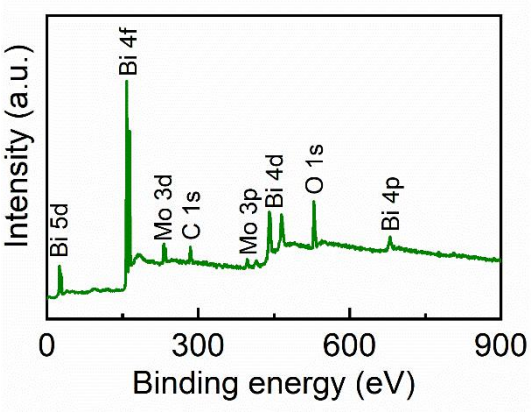

Fig. S3. The XPS survey spectrum of the Bi_2MoO_6 nanopillars.

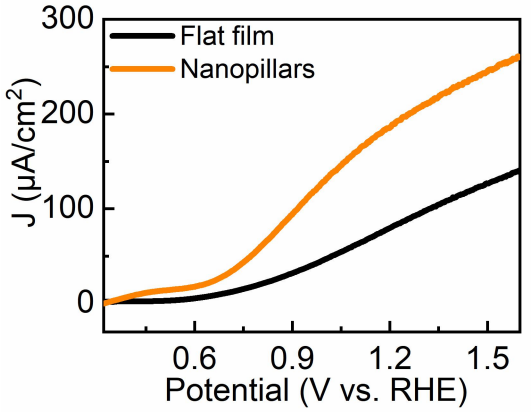

Fig. S4. *J-V* curves of the flat Bi_2MoO_6 film and the Bi_2MoO_6 nanopillars.

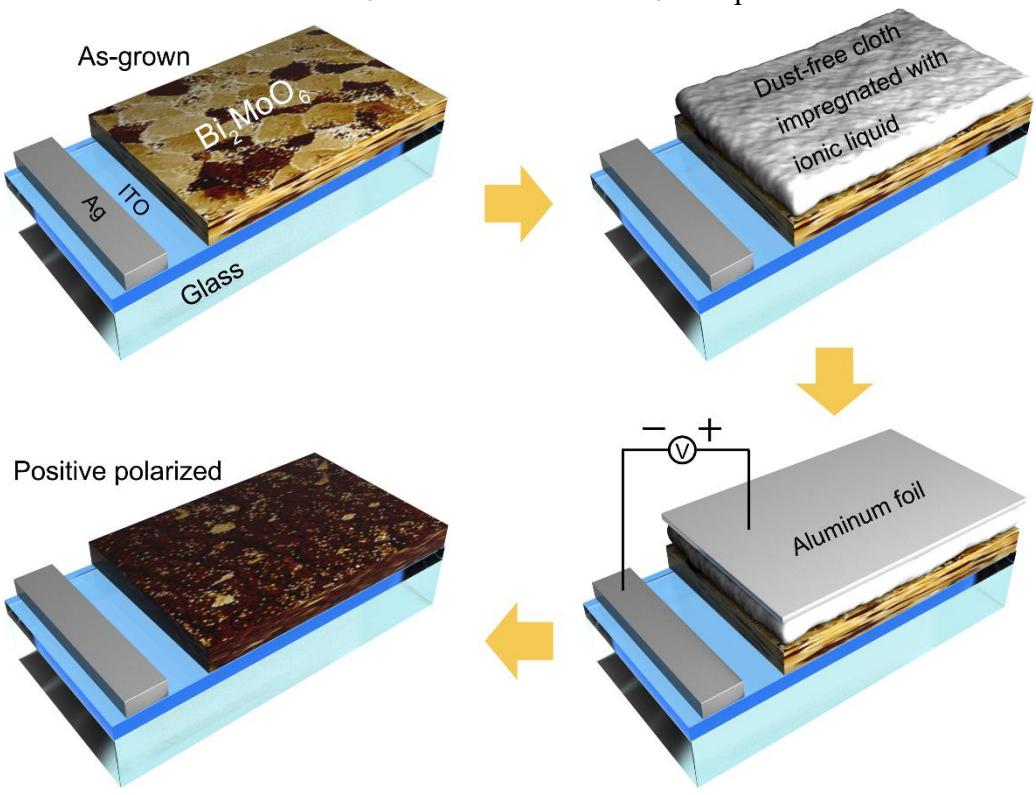

Fig. S5. Schematic diagrams about the polarization poling process of Bi_2MoO_6 nanopillars with ionic

liquid as top electrode.

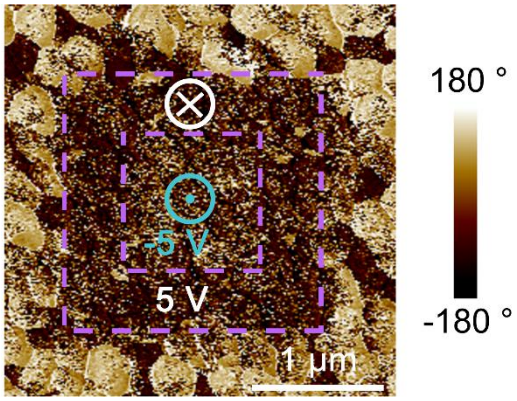

Fig. S6. Out-of-plane PFM image of the Bi_2MoO_6 nanopillars polarized by the conductive tip with -5 V and 5V, respectively.

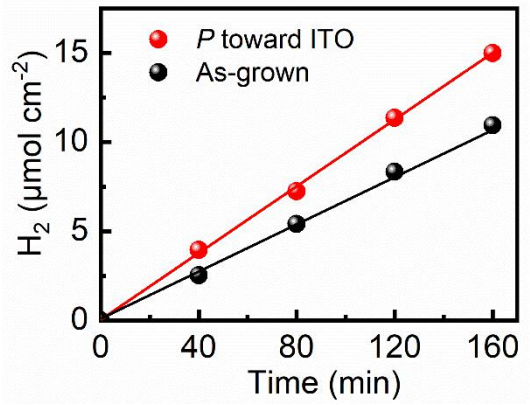

Fig. S7. Dependence of H_2 amount on lighting time of the as-grown sample and that with polarization toward ITO recorded at 1.1 V vs. RHE in the 0.5 M Na_2SO_4 and 0.2 M Na_2SO_3 aqueous solution.

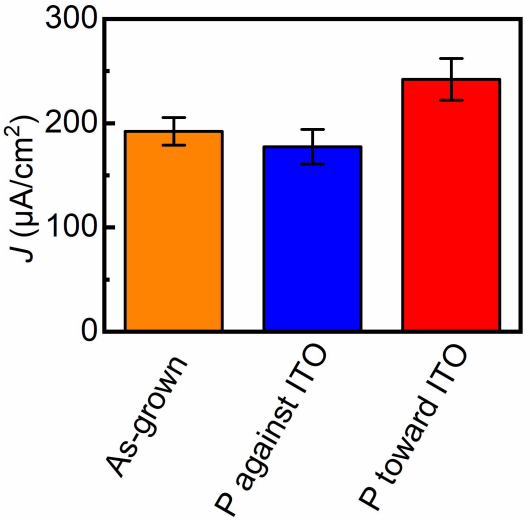

Fig. S8. Photocurrent density of Bi_2MoO_6 photoanodes with three different polarization statuses at 1.23 V vs. RHE under AM 1.5 G solar light illumination (100 mW cm^{-2}).

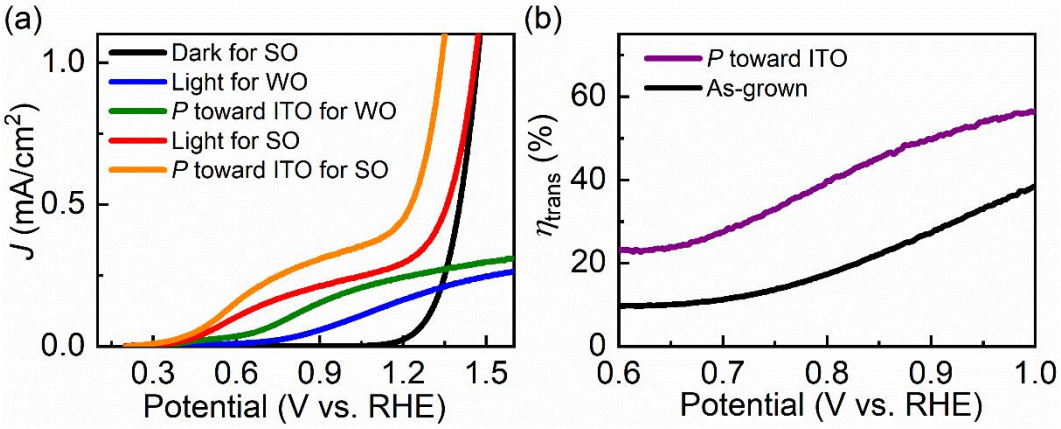

Fig. S9. (a) Comparison of *J-V* curves of Bi_2MoO_6 photoanodes measured for water oxidation (WO) in 0.5 M Na_2SO_4 aqueous solution and for sulfite oxidation (SO) in the 0.5 M Na_2SO_4 and 0.2 M Na_2SO_3 aqueous solution. (b) Charge transfer efficiency (η_{trans}) of the as-grown Bi_2MoO_6 nanopillars without macroscopic polarization and that with the macroscopic polarization toward ITO electrode, where J_{Ph} is the photocurrent density measured in the Na_2SO_4 aqueous solution, J_{HS} is the photocurrent density measured in the 0.5 M Na_2SO_4 and 0.2 M Na_2SO_3 aqueous solution, and η_{trans} is J_{Ph}/J_{HS}.

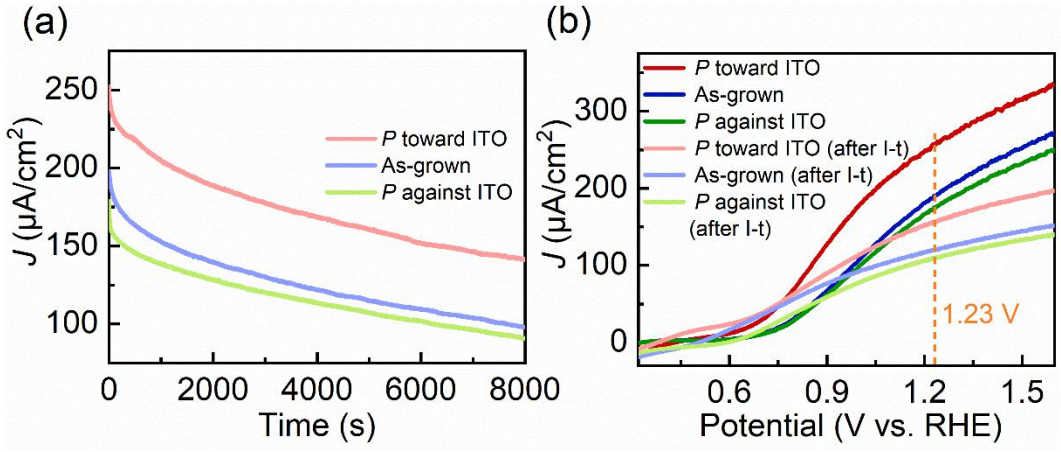

Fig. S10. (a) Stability test of three-type Bi_2MoO_6 photoanodes (as-grown, P toward ITO, and P against ITO) at 1.23 V vs. RHE, and (b) their photoelectrochemical properties before and after above stability test.

References

1. X. Zhao, T. Xu, W. Yao and Y. Zhu, *Thin Solid Films*, 2009, **517**, 5813-5818.
2. M. Wu, Y. Wang, Y. Xu, J. Ming, M. Zhou, R. Xu, Q. Fu and Y. Lei, *ACS Appl. Mater. Interfaces*, 2017, **9**, 23647-23653.
3. Y. Ma, Y. Jia, L. Wang, M. Yang, Y. Bi and Y. Qi, *Phys. Chem. Chem. Phys.*, 2016, **18**, 5091-5094.
4. L. Wang, R. Wang, Y. Zhou, Q. Shen, J. Ye, C. Wu and Z. Zou, *Catal. Today*, 2019, **335**, 262-268.
5. J. Zhang, T. Wang, X. Chang, A. Li and J. Gong, *Chem. Sci.*, 2016, **7**, 6381-6386.